



## Length dependence of coercivity in CoFe<sub>2</sub> nanowire arrays with high aspect ratios

S.L. Lim<sup>a</sup>, F. Xu<sup>b</sup>, N.N. Phuoc<sup>b</sup>, C.K. Ong<sup>a,\*</sup>

<sup>a</sup> Physics Department, National University of Singapore, Singapore 117542, Singapore

<sup>b</sup> Temasek Laboratories, National University of Singapore, Singapore 117411, Singapore

### ARTICLE INFO

#### Article history:

Received 4 December 2009

Received in revised form 10 June 2010

Accepted 12 June 2010

Available online 25 June 2010

#### Keywords:

CoFe<sub>2</sub> nanowires

AAO template

Magnetostatic interaction

Coercivity

Length dependence

### ABSTRACT

CoFe<sub>2</sub> nanowires with high aspect ratios were electrodeposited into the anodic aluminum oxide (AAO) template. The coercivities and remanence measured along the longitudinal axis of the nanowires are found to increase with the length of nanowires. The magnetostatic interaction between the nanowires is responsible for the decrease of coercivity and remanence of an array of nanowires as compared to an isolated single nanowire. By considering the magnetostatic interaction between the nanowires, a simple model as a function of length is used to calculate the coercivity in an array of the nanowire and this model shows good agreement with experimental data.

Crown Copyright © 2010 Published by Elsevier B.V. All rights reserved.

### 1. Introduction

Highly ordered arrays of magnetic nanowires have potential applications in new magnetic devices and particularly in recording media [1,2]. The high ordering and intrinsic nature of the nanomagnets give rise to outstanding cooperative properties which are of fundamental and technological interest [3]. As a result, the magnetic properties of magnetic nanowires have been widely researched on. Electrodeposition of magnetic nanowires into anodic aluminum oxide (AAO) template is one of the most popular approaches to fabricate magnetic nanowires. This method offers many advantages, such as low cost, high yield and fine control over the length and diameter of the nanowires [4].

Studies on general magnetic behaviors have been reported on nanowire arrays of Fe, Ni, Co and their alloys [5–7]. The magnetic properties of the nanowires are governed by two factors, the magnetic nature of the individual nanowire and the magnetostatic interactions between the nanowires. The magnetic nature of individual nanowire is influenced by the longitudinal uniaxial shape, magnetocrystalline and magnetoelastic anisotropies. The magnetostatic interaction originates from unbalanced magnetic poles at both ends of individual wires generating stray fields that couple with the magnetization of neighboring nanowires. Magnetostatic interactions can reduce the switching field of the nanowires as compared to the non-interacting array of nanowires. With

magnetostatic interactions considered, previous works have well interpreted the decreases of coercivity and remanence of nickel nanowire arrays with the increase of diameter of the nanowires while their interpore distance is kept constant [8,9].

In this paper, we investigate the length dependence of the coercivity of CoFe<sub>2</sub> nanowire arrays which have the high aspect ratios ranging from 200 to 1000. Few experimental works have been carried on this issue in detail and in this range of aspect ratio [10,11]. The coercivity of the nanowires in this work cannot be explained based on the assumption of non-interacting nanowires. The magnetostatic interaction between the nanowires is included to account for the length dependence of the nanowire arrays. A simple model based on the influence of the effective magnetostatic energy is used to calculate the coercivity of the nanowires and the calculation with this model shows a good agreement with experimental data.

### 2. Experiment

The AAO templates were prepared from aluminum foil by one-step anodization technique. The aluminum foils were cleaned by ultrasonic in acetone and distilled water before they were annealed in furnace for 6 h at 500 °C. Then, the annealed aluminum foils were electropolished at 20 V for 2 min in a solution consisting of ethanol and perchloric acid at a ratio of 5:1. The electropolishing was carried out at temperature of 5 °C. After this treatment, the aluminum foils were anodized at 25 V in 0.4 M H<sub>2</sub>SO<sub>4</sub> at 10 °C to form AAO template. The lengths of the AAO templates were varied from 7 μm to 35 μm by using different anodizing time. The pore diameter and the distance between two nearest pores of the AAO template were kept constant. The AAO templates were immersed in 0.3 M H<sub>3</sub>PO<sub>4</sub> for 15 min at 40 °C to widen the pore and to thin down the barrier layer so that it was suitable for AC electrodeposition. CoFe<sub>2</sub> nanowires were deposited into AAO templates by AC electrodeposition. The electrolyte used in the AC electrodeposition consisted of 0.073 M CoSO<sub>4</sub>, 0.0147 M FeSO<sub>4</sub>, 0.6 M boric acid and 1 g/L of ascorbic acid. Deposition was carried out at room temperature with an AC voltage of 16 V, 100 Hz using graphite rod as counter elec-

\* Corresponding author. Tel.: +65 65162984; fax: +65 67776126.

E-mail address: [phyongck@nus.edu.sg](mailto:phyongck@nus.edu.sg) (C.K. Ong).

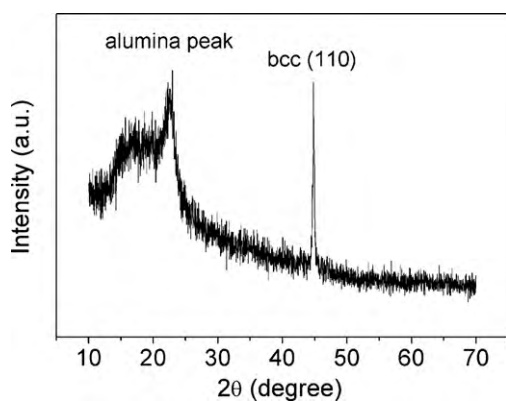


**Fig. 1.** XRD pattern of the CoFe<sub>2</sub> nanowires embedded in the AAO template with the aluminum removed.

trode. The current of the deposition was monitored during the deposition. Initially, the current fell sharply and then remained stable. The deposition of the nanowires was stopped when there was an increase in the current, indicating that some of the nanowires were growing out of the AAO template.

The microstructure of the AAO template and nanowires were observed by scanning electron microscopy (SEM) and by transmission electron microscopy (TEM), respectively. The length of AAO template was measured by cutting the AAO template with a pair of scissor for the SEM side view of the template. In order to measure the length of CoFe<sub>2</sub> nanowires deposited in the AAO template, the AAO template was first etched in a solution of 6 wt% H<sub>3</sub>PO<sub>4</sub> and 1.8 wt% CrO<sub>3</sub> at 40 °C until the tip of the nanowires were exposed. Then the AAO template filled with CoFe<sub>2</sub> nanowires was cut with a pair of scissor for the SEM side view. To liberate the nanowires from the templates for TEM studies, the AAO template was dissolved in 1 M NaOH. After this, the solution was washed carefully with distilled water for several times, and then a drop of suspension was dropped on a copper grid coated with carbon film for TEM observation. The phase structure of the nanowires was investigated by X-ray diffraction (XRD) with Cu K $\alpha$  radiation and selected area electron diffraction (SAED) of the TEM. Prior to the XRD measurement, the aluminum was removed from the AAO template embedded with CoFe<sub>2</sub> nanowires using CuCl<sub>2</sub> solution. The magnetic properties of the nanowires were measured by vibrating sample magnetometer (VSM) with the applied field parallel to the long axis of wires.

### 3. Results and discussions

The crystallographic structure of the CoFe<sub>2</sub> nanowires was examined using the XRD. Fig. 1 displays the typical XRD spectra of the electrodeposited CoFe<sub>2</sub> nanowires embedded in the AAO template. CoFe<sub>2</sub> nanowires exhibit body-centered cubic structure with a preferred texture orientation of [1 1 0] along the long axis of nanowires.

The SEM image of the AAO template is shown in Fig. 2(a). And it shows that the average pore diameter pore is 32 nm and the inter-pore distance ( $D$ ) is 65 nm. The SEM top view of 21  $\mu$ m long AAO template deposited with CoFe<sub>2</sub> nanowires which has been etched in a solution of 6 wt% H<sub>3</sub>PO<sub>4</sub> and 1.8 wt% CrO<sub>3</sub> at 40 °C is presented in Fig. 2(b). Clearly the tips of the nanowires are exposed from etching of the AAO template. The corresponding SEM side view of the same AAO template filled with CoFe<sub>2</sub> nanowires is shown in Fig. 2(c). Fig. 2(c) shows that the length of the nanowires is about 20.5  $\mu$ m which is close to the length of the AAO template in which the nanowires is deposited. Fig. 2(d) shows the enlarged view of Fig. 2(c). Fig. 3 shows the TEM image of the CoFe<sub>2</sub> nanowires freed from the AAO template. The diameter of the CoFe<sub>2</sub> nanowires ( $2R$ ) is also 32 nm which is consistent with the average pore diameter of AAO template. The polycrystalline structure of the CoFe<sub>2</sub> nanowires was confirmed by the multiple diffraction rings in the SAED of TEM.

Fig. 4(a) presents the magnetic hysteresis loops of the nanowire arrays with the average nanowire length ( $L$ ) varying from 7  $\mu$ m to 35  $\mu$ m with the field applied parallel to the long axis of nanowires. Fig. 4(b) shows the magnetic hysteresis loops of the nanowire arrays with the field applied perpendicular to the long

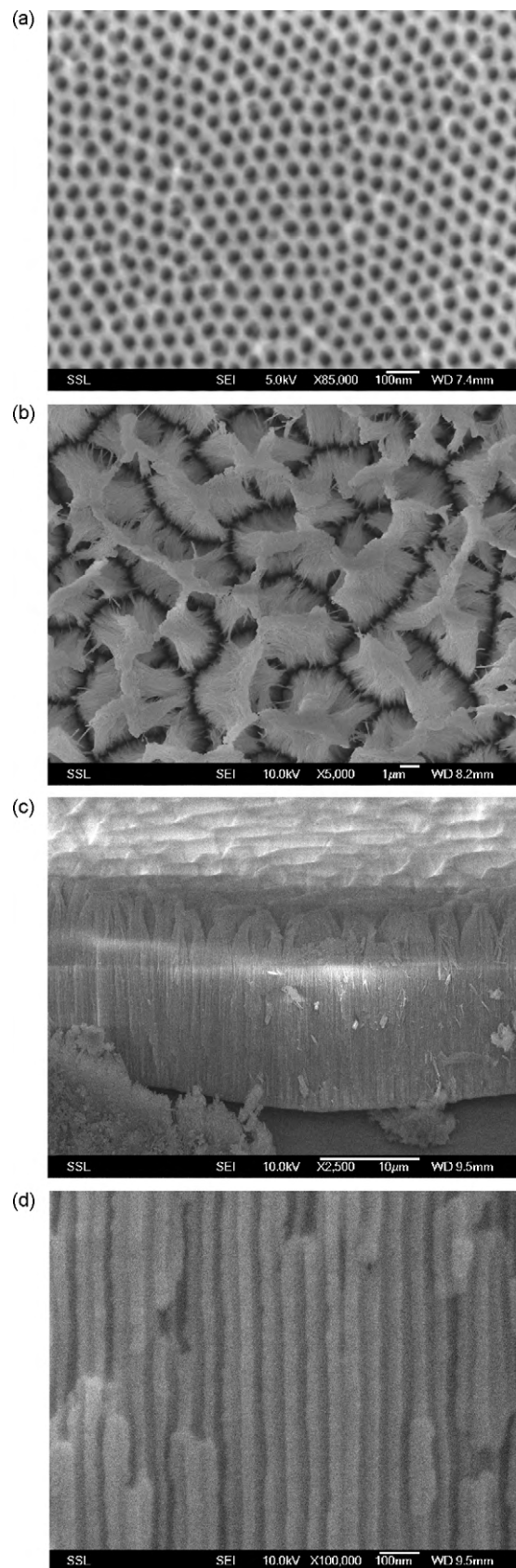


**Fig. 2.** (a) SEM Picture of the top view of the AAO template fabricated. (b) The SEM top view of 21  $\mu$ m long AAO template deposited with CoFe<sub>2</sub> nanowires which has been etched in a solution of 6 wt% H<sub>3</sub>PO<sub>4</sub> and 1.8 wt% CrO<sub>3</sub> at 40 °C. (c) The corresponding SEM side view of the same AAO template filled with CoFe<sub>2</sub> nanowires. (d) The enlarged SEM view of (c).

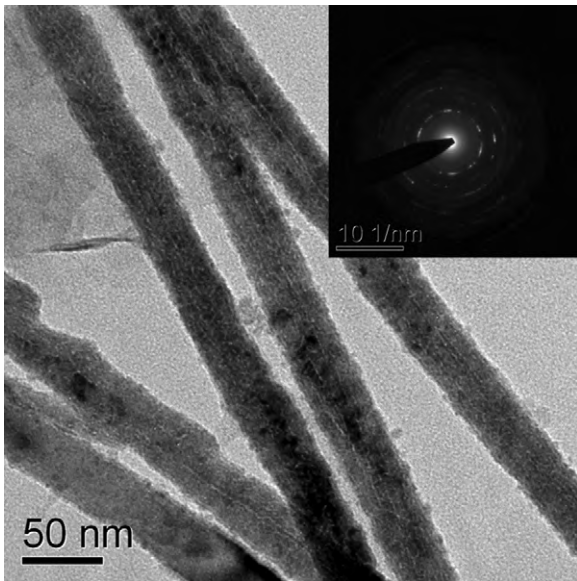


**Fig. 3.** TEM picture of the CoFe<sub>2</sub> nanowires freed from the AAO template with the inset showing the SAED of the CoFe<sub>2</sub> nanowires.

axis of nanowires. The comparison of these loops clearly shows the increase of coercivity with the length. The magnetic properties of an isolated nanowire have been also studied with the micromagnetism simulation based on the Landau–Lifshitz–Gilbert equation. LLG Micromagnetics Simulator™ is used to simulate the hysteresis loop of an isolated CoFe<sub>2</sub> nanowire with applied field parallel to the long axis of nanowire. The cell size is chosen to be 8 nm × 8 nm × 8 nm and the damping factor is 0.3. The saturation

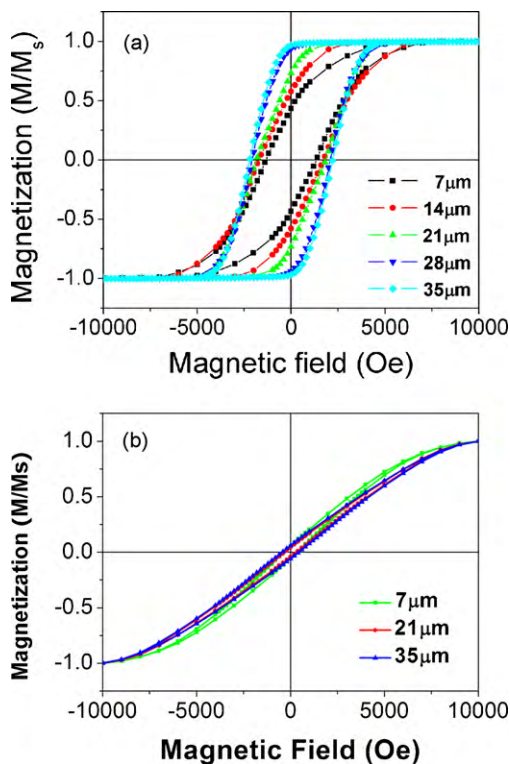


**Fig. 4.** (a) Hysteresis loops of the CoFe<sub>2</sub> nanowires with length  $L$  varying from 7  $\mu\text{m}$  to 35  $\mu\text{m}$ . The external field is applied parallel to the long axis of the nanowires. (b) Hysteresis loops of the CoFe<sub>2</sub> nanowires with the external field applied perpendicular to the long axis of the nanowires.

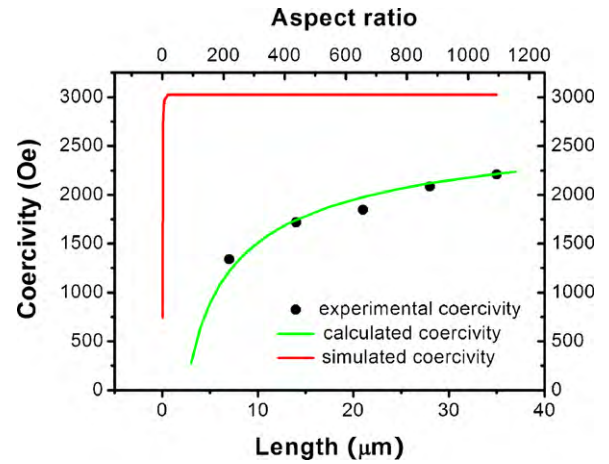


**Fig. 5.** Coercivity of the nanowires as a function of length. The red line represents the LLG simulation result of the coercivity of an isolated nanowire. The green line represents the coercivity in an array of CoFe<sub>2</sub> nanowires calculated using Eq. (1). The black dots are the experimental results of coercivity measured by VSM. (For interpretation of the references to color in this figure legend, the reader is referred to the web version of the article.)

magnetization of CoFe<sub>2</sub> nanowires ( $M_s$ ) is 1930 emu/cm<sup>3</sup> and the exchange constant is  $2.5 \times 10^{-11}$  J/m. Since the CoFe<sub>2</sub> nanowire has a polycrystalline structure, the crystalline anisotropy energy is chosen to be zero. The coercivity of a long wire with large radius can also be predicted from curling mode [12],  $H_0 = cA/\mu_0 M_s R^2$  and is calculated to be 3430 Oe. However, the coercivity of a long wire from the simulation is 3025 Oe which is much lower than that predicted by the curling mode. Fig. 5 presents the experimental and simulation results of length dependence of coercivity. Clearly, the shape anisotropy of an isolated nanowire cannot account for the trend of increasing coercivity with the length at high aspect ratio ranging from 200 to 1000.

In order to interpret this behavior, magnetostatic interaction between the nanowires must be taken into consideration when the distance between two nearest nanowires is comparable to the diameter of a nanowire. Stray field generated from each nanowire in the array will couple with the magnetizations of other nanowires. This magnetostatic interaction favors an anti-parallel distribution of magnetization in neighboring nanowires [8,13]. In an array with all the nanowires initially magnetized in the same direction, the magnetostatic interaction between neighboring nanowires favors the reversal of some of them. Assuming the reversal of an individual nanowire produces a decrease of magnetostatic interaction  $\varepsilon E_{\text{int}}(D)$  that equals to the magnetic anisotropy barrier  $\Delta E$  of a nanowire, the macroscopic coercivity will be:

$$H_c = H_0 \left( 1 - \sqrt{\frac{\varepsilon E_{\text{int}}(D)}{K_1 V}} \right) \quad (1)$$

where  $V$  represents the volume of a single nanowire and  $H_0$  is the coercivity of an isolated nanowire,  $E_{\text{int}}(D)$  represents the magnetostatic interaction between two nanowires separated by distance  $D$ . Such interaction has been derived by assuming the homogeneous magnetization in the direction along long axis of the wire and has the expression  $E_{\text{int}} = \mu_0 M_s^2 R^2 / 2DL [1 - (1/\sqrt{1 + L^2/D^2})]$  if the  $R/L \ll 1$  [14]. Assuming that the each magnetic nanowire is single domain and has the uniaxial shape anisotropy, magnetic anisotropy barrier will be given as  $\Delta E = K_1 V (1 - H/H_0)^2$ , with the uniaxial shape anisotropy  $K_1 = \mu_0 M_s H_0 / 2$  [15]. Finally, the macroscopic coercivity as a function of  $L$  can be expressed as  $H_c = H_0 [1 - \sqrt{\varepsilon M_s R^2 / H_0 D L (1 - (1 + L^2/D^2)^{-1/2})}]$ . Moreover,  $\varepsilon$  is a fitting parameter that depends on the distribution magnetic wires

in space and on the long distance correlation among the wires. In Eq. (1), both  $H_0 = 3025$  Oe which is obtained from the LLG simulation and  $\varepsilon = 80$  are used. Since the magnetostatic energy  $E_{\text{int}}(D)$  decreases with length of nanowires, the coercivity in the array of CoFe<sub>2</sub> nanowires increases with the length of nanowires. The calculated coercivity is presented in Fig. 5. It can predict the trend observed in the experimental data and shows relatively good agreement with experimental data. At lower shape ratio range, Vázquez et al. studied the effect of length on the coercivity and observed that there was almost a linear relationship between the coercivity and length [10]. On the contrary, in dot arrays where  $2R > L$ , a different behavior is observed in which case the coercivity decreases with increasing length [16].

Not only the coercivity of the nanowires increases with the length of nanowires, the remanence ( $M_r/M_s$ ) is also observed to increase with the length of the nanowires from Fig. 5. This can be explained by the length dependence of the magnetostatic interaction between the nanowires. As the length of the nanowires interaction increases, the magnetostatic interaction decreases. Thus the anti-parallel configuration between the magnetization states of the nanowires becomes less favorable and fewer nanowires have their magnetization flipped in the opposite direction in zero applied field.

#### 4. Conclusion

In conclusion, we have fabricated CoFe<sub>2</sub> nanowires with high aspect ratios to investigate the effect of length on the coercivity and remanence. From the VSM measurements, the coercivity and remanence increase with the length of the nanowires. In order to account for such a phenomenon, the effect of magnetostatic interaction between the nanowires due to the coupling of stray field with the magnetization of nanowires must be included. This magnetostatic interaction will reduce the coercivity and remanence in the

array of nanowires. For longer length of nanowires, the strength of magnetostatic interaction becomes weaker and thus the coercivity and remanence increase. A simple expression as a function of magnetostatic interaction is used to obtain the coercivity in an array of CoFe<sub>2</sub> nanowires and shows relatively good agreement with the coercivity measured by the VSM.

#### Acknowledgment

This research was financially supported by Defense Science and Technology Agency of Singapore. And the authors would like to acknowledge Dr. D.H. Wang and Prof. S.G. Yang for the instruction of sample preparations.

#### References

- [1] G. Prinz, *Science* 282 (1998) 1660.
- [2] R.P. Cowburn, M.E. Welland, *Science* 287 (2000) 1466.
- [3] R. Skomski, H. Zeng, M. Zheng, D.J. Sellmyer, *Phys. Rev. B* 62 (2000) 3900.
- [4] H. Masuda, K. Fukuda, *Science* 268 (1995) 1466.
- [5] D.J. Sellmyer, M. Zheng, R. Skomski, *J. Phys.: Condens. Matter* 13 (2001) R433.
- [6] P.M. Paulus, F. Luis, M. Kröll, G. Schmid, L.J. de Jongh, *J. Magn. Magn. Mater.* 224 (2001) 180.
- [7] K. Nielsch, R.B. Wehrspohn, J. Barthel, J. Kirschner, S.F. Fischer, H. Kronmüller, T. Schweinböck, D. Weiss, U. Gösele, *J. Magn. Magn. Mater.* 249 (2002) 234.
- [8] M. Vázquez, K. Pirota, M. Hernández-Vélez, V.M. Prida, D. Navas, R. Sanz, F. Batallán, J. Velázquez, *J. Appl. Phys.* 95 (2004) 6642.
- [9] K. Nielsch, R.B. Wehrspohn, J. Barthel, J. Kirschner, U. Gösele, S.F. Fischer, H. Kronmüller, *Appl. Phys. Lett.* 79 (2001) 1360.
- [10] M. Vázquez, K. Pirota, J. Torrejón, D. Navas, M. Hernández-Vélez, *J. Magn. Magn. Mater.* 294 (2005) 174.
- [11] J. Escrig, R. Lavín, J.L. Palma, J.C. Denardin, D. Altbir, A. Cortés, H. Gómez, *Nanotechnology* 19 (2008) 075713.
- [12] R. Skomski, J.P. Liu, D.J. Sellmyer, *Phys. Rev. B* 60 (1999) 7359.
- [13] M. Bahiana, F.S. Amaral, S. Allende, D. Altbir, *Phys. Rev. B* 74 (2006) 174412.
- [14] D. Laroze, J. Escrig, P. Landeros, D. Altbir, M. Vázquez, P. Vargas, *Nanotechnology* 18 (2007) 415708.
- [15] M.P. Sharrock, *J. Appl. Phys.* 76 (1994) 6413.
- [16] M. Grimsditch, Y. Jaccard, I.K. Schuller, *Phys. Rev. B* 58 (1998) 11539.